THE ASTROPHYSICAL JOURNAL, 497:330–341, 1998 April 10

CANDIDATE MAIN-SEQUENCE STARS WITH DEBRIS DISKS: A NEW SAMPLE OF VEGA-LIKE SOURCES

VINCENT MANNINGS
Division of Physics, Mathematics and Astronomy, California Institute of Technology, MS 105-24, Pasadena, CA 91125
AND
MICHAEL J. BARLOW
Department of Physics and Astronomy, University College London, Gower Street, London WC1E 6BT, UK
Received 1996 July 24; accepted 1997 November 17

ABSTRACT

Vega-like sources are main-sequence stars that exhibit IR fluxes in excess of expectations for stellar photospheres, most likely due to reradiation of stellar emission intercepted by orbiting dust grains. We have identified a large sample of main-sequence stars with possible excess IR radiation by cross-correlating the Michigan Catalog of Two-dimensional Spectral Types for the HD Stars with the *IRAS* Faint Source Survey Catalog. Some 60 of these Vega-like sources were not found during previous surveys of the *IRAS* database, the majority of which employed the lower sensitivity Point Source Catalog. Here, we provide details of our search strategy, together with a preliminary examination of the full sample of Vega-like sources.

Subject headings: circumstellar matter — infrared: stars

1. INTRODUCTION

Vega-like sources are main-sequence stars with disks or rings of orbiting dust grains. These circumstellar structures may be the evolved remnants of once massive disks, perhaps augmented by debris products generated during the ongoing disruption of planetesimal-sized bodies (cf., Backman & Paresce 1993, and references therein). The disks represent an important end state for material that has survived—and is being replenished—long after the termination of the protostellar collapse phase, and beyond the (presumed) era of planet formation, too. The detailed study of the composition, size, and spatial distribution of the dust grains comprising these disks therefore promises rich insight to the processes by which planetary systems are created.

Aumann (1985) restricted the adjective "Vega-like" to main-sequence stars with flux densities at 60 μm that are in excess of the levels expected for stars of their spectral types, as evidenced during all-sky survey measurements with the *Infrared Astronomical Satellite* (*IRAS*). We will use the term "Vega-like" more flexibly here to describe a main-sequence star that exhibits excess flux at any *IRAS* infrared (IR) wavelength.

The eponymous star Vega (α Lyr) was serendipitously found by Aumann et al. (1984) to be approximately 1 order of magnitude brighter at far-IR wavelengths than expected for an A0 V star. The additional flux was ascribed to radiation from grains in thermal equilibrium with the stellar radiation field, and distributed within a shell or ring with an inner radius of several tens of AU. Shortly after this discovery the A5 V star β Pic, also found to have excess far-IR emission (Gillett 1986), was observed with an optical coronagraph by Smith & Terrile (1984), revealing a highly inclined dust-scattering disk extending out to hundreds of AU from the star.

The *IRAS* measurements were the first to identify excess IR emission from main-sequence stars that are not undergoing significant mass loss from their surfaces. Subsequently, many programs of study have sought to understand the Vega-like stars within the context of the end products of the evolution of circumstellar disks associated with pre–main-sequence stars, the possible formation of planetesimals and planets, and perhaps even the disruption of infalling cometary bodies. See the reviews by Backman & Paresce (1993) and Lagrange-Henri (1995), and see also Vidal-Madjar & Ferlet (1994). Despite attempts to image the material around many other Vega-like sources (e.g., Smith, Fountain, & Terrile 1992; Kalas & Jewitt 1996), only one further star, BD $+31°643$ (Kalas & Jewitt 1997) has joined β Pic in the select group for which the circumstellar material has been imaged directly at optical wavelengths. (Skinner et al. 1995 have imaged a dust structure around SAO 26804 at $\lambda \approx 10$ μm.) Our information on the nature of most Vega-like sources has instead been gleaned indirectly from ground-based optical and near- and mid-IR spectroscopy and by combining the *IRAS* measurements with ground-based near-IR and millimeter-wave photometry for studies of the continuum spectral energy distributions. In these ways the composition of grains, together with their temperature, size, spatial distribution, and total mass, have all been probed (Chini et al. 1991; Telesco & Knacke 1991; Skinner, Barlow, & Justtanont 1992; Aitken et al. 1993; Knacke et al. 1993; Zuckerman & Becklin 1993; Sylvester, Barlow, & Skinner 1994a, 1994b; Skinner et al. 1995; Sylvester et al. 1996).

At the same time, various searches of the *IRAS* catalogs have been made to try to identify new candidate Vega-like stars (see below for a summary). In the present work we provide the results of a new search of the *IRAS* Faint Source Survey Catalog (Moshir et al. 1989) for associations of IR sources with Southern Hemisphere main-sequence stars listed in the current version of the Michigan Catalog of Two-dimensional Spectral Types for the HD Stars. Multiband near- to far-IR photometry of a subset of these Vega-like candidates is being obtained using the *Infrared Space Observatory* (*ISO*), and we have an ongoing program of ground-based observations. These measurements will be discussed in a forthcoming set of papers. Here we provide

preliminary details of the full set of Vega-like stars identified in the Michigan catalog. In § 2 we briefly describe earlier searches of the *IRAS* data. The database employed for the present work is described in § 3, together with the criteria used to select Vega-like sources and the method employed to identify excess mid- and far-IR fluxes. The results are tabulated and described in § 4. Our search method is compared in § 5 to those employed in some previous surveys of the *IRAS* catalogs, and we discuss our results in § 6.

2. PREVIOUS SURVEYS

At least a dozen searches have been made through the *IRAS* database for evidence of IR sources associated with samples of objects that include stars on the main sequence. These are summarized in Table 1. Most employed the *IRAS* Point Source Catalog, which provides flux densities measured in four wavelength bands centered approximately at 12, 25, 60, and 100 μm, and were limited to particular spectral types and to bright and/or nearby stars. We will briefly mention the larger surveys here.

The first major search (Walker & Wolstencroft 1988) used both the full SAO catalog and the Catalog of Nearby Stars (Gliese 1969), and included the selection criterion that potential candidates have a 60:100 μm flux density ratio similar to that of the prototype Vega-like stars. All selected sources were further required to exhibit evidence for extended emission in one or more of the *IRAS* photometric bands. Of the resulting set of just 34 stars, only half are known to be on the main sequence. By relaxing both these restrictions, Stencel & Backman (1991) identified a total of 379 SAO stars with apparent IR excesses but, again, main-sequence dwarfs comprised only a subset. (See also § 5 below). Oudmaijer et al. (1992) made a similar survey of all luminosity classes, but with the exclusion of stars with spectral type K and later. (See § 5). Backman & Paresce (1993) have compiled a list of 54 main-sequence stars with mid- and far-IR excesses, culled from several of the surveys noted in Table 1.

3. THE NEW SEARCH FOR VEGA-LIKE SOURCES

3.1. *The Database*

The aim of the present work is to make a systematic search for *main-sequence* stars with IR excesses using the *IRAS* Faint Source Survey Catalog (Moshir et al. 1989, hereafter FSC), which contains information on 173,044 sources in the relatively unconfused regions of sky at Galactic latitudes $|b| \geq 10°$, corresponding to approximately 80% of the sky. The FSC has the best limiting sensitivity of all the available *IRAS* data products and is approximately 1 mag more sensitive than the *IRAS* Point Source Catalog, Version 2, 1988 (hereafter PSC) as a result of co-adding the full set of point-source–filtered individual detector scans of any given sky region, in each of the four wavelength bands.

To work with a large sample of stars with accurately determined luminosity classifications, we have used digitized versions of the four released volumes of the Michigan Catalog of Two-dimensional Spectral Types for the HD Stars, which we shall henceforth refer to as the Michigan Spectral Catalog (MSC: Houk & Cowley 1975; Houk 1978, 1982; Houk & Smith-Moore 1988; Houk 1994). This ongoing survey provides information on the spectral types and luminosity classes—the two "dimensions" in the name of the catalog—of some 130,397 HD stars in the declination range $\delta = -90°$ to $-12°$. Although the four volumes of the MSC published to date cover less than 50% of the sky, they include 58% of the stars in the HD catalog (Houk 1994), due to the offset of the Galactic center to southern declinations. This potential advantage is, however, offset by the likelihood that the majority of the main-sequence stars found by our sampling method are relatively nearby, so that Volumes 1–4 of the MSC may only contain about 50% (or less) of the main-sequence stars having infrared excesses that are potentially extractable from the *IRAS* FSC. For each star, the MSC records the designation in the HD catalog, the newly determined spectral type and luminosity class, the photographic V-band magnitude, and the equatorial and Galactic coordinates. Equatorial coordinates are provided for equinox 1900. Also given are the centennial precessions in right ascension and declination, which we have used to transform all equatorial coordinates to equinox 1950, for consistency with the equinox adopted for the *IRAS* catalogs. (Spot checks of the results of these transformations were made by comparing to corresponding entries in the SAO catalog—equinox 1950.0—and the precessed coordinates were found to be consistent.) The equatorial coordinates listed in Volume 1 of the MSC (Houk & Cowley 1975) are taken directly from the original HD catalog and are not sufficiently precise for our purposes:

TABLE 1

PREVIOUS SURVEYS OF THE *IRAS* DATA CATALOGS

Authors	Database	Comments
Aumann 1985	PSC,[a] Catalog of Nearby Stars	Identified eight new Vega-like stars
Jaschek, Jaschek, & Egret 1986	PSC, Catalog of Stellar Groups	Ae/A-type shell stars only
Johnson 1986	PSC, compilation of dKe stars	K Ve stars only
Odenwald 1986	PSC, various compilations	G-type stars only, including dwarfs
Sadakane & Nishida 1986	PSC, Bright Star Catalog	12 new Vega-like stars identified
Coté 1987	PSC, Bright Star Catalog	B and A stars only
Walker & Wolstencroft 1988	PSC, SAO, Catalog of Nearby Stars	Search for sources with *IRAS* colors of prototypes
Aumann & Probst 1991	PSC, Catalog of Nearby Stars	Search for 12 μm excesses
Patten & Willson 1991	PSC, MSC, Bright Star Catalog, Catalog of Stellar Rotational Velocities	Main-sequence B, A, and F stars
Stencel & Backman 1991	PSC, SAO	Included B, A, F, G, K, and M stars of all luminosity classes
Cheng et al. 1992	FSC, Bright Star Catalog, Catalog of Stars within 25 pc of the Sun	Main-sequence A-type stars only
Oudmaijer et al. 1992	PSC, SAO	Included B, A, F, and G stars of all luminosity classes

[a] *IRAS* Point Source Catalog.

right ascension is given to an accuracy of 0.1 minute of time, and declination to 1′. (Volumes 2–4 provide positions that are accurate to 0.1 s in right ascension, and to 1″ in declination.) We have cross-correlated the records in Volume 1 (according to HD designation) with the SAO catalog in order to exploit the accurate coordinates provided by the latter. The resulting subset (52%)[1] of Volume 1 stars is used together with Volumes 2–4 throughout the present work, providing a combined set of 112,971 stars.

3.2. *Procedure for Identification of Sources*

To be considered as Vega-like candidates, associations of MSC stars with FSC IR sources are required to satisfy the following criteria:

1. The separation on the sky must be $\leq 60''$. As a result, 83% of MSC stars are rejected, leaving 19,480 in total.
2. The quality of the *IRAS* flux densities of the position-associated sources must be flagged in the FSC as either "excellent" or "moderate," which correspond respectively to "FQUAL" flags 3 and 2. (FQUAL = 1 signifies a nondetection.) To avoid spurious associations with Galactic "cirrus" emission at 60 and 100 μm, we accept only candidates with excellent/moderate detections in one of the following combinations of wavelength bands: (*a*) 12, 25, and 60 μm (*b*) 12 and 25 μm (*c*) 25 and 60 μm. On these criteria, a further 14,158 MSC stars are rejected, producing a subset of 5322 sources.
3. To restrict ourselves to main-sequence stars, we next reject those sources with MSC luminosity classifications in the range I–IV. A small subset of 294 MSC/FSC candidates for which the MSC claims a luminosity class of V then remains. Note that we exclude from this subset all sources for which a main-sequence classification is uncertain, i.e., those classed in the MSC as III/V or IV/V.
4. Finally, we are left with just 131 stars after rejecting 163 luminosity class V MSC stars that fail to exhibit significant IR flux excesses above the photospheric values expected at or longward of $\lambda = 12$ μm. The scheme for defining these excesses is described below.

3.3. *Method for Testing for Excess IR Emission*

Let the 12, 25, and 60 μm flux densities listed in the FSC for any given source be F_{12}, F_{25}, and F_{60}, respectively. We consider the two ratios of flux densities defined by

$$R_{12/25} \equiv \frac{F_{12}}{F_{25}} \tag{1}$$

and

$$R_{25/60} \equiv \frac{F_{25}}{F_{60}} . \tag{2}$$

By comparing the ratios of measured flux densities to the ratios expected for a star of given spectral type, we have a simple and straightforward method for automating the rejection of those stars without significant mid- to far-IR excesses.[2] We know from the FSC the (independent) uncertainties, δF, on each of the *IRAS* flux densities, so that we immediately obtain an expression for the error on the observed 12:25 μm ratio:

$$\delta R_{12/25} = \pm \frac{F_{12}}{F_{25}} \sqrt{\left(\frac{\delta F_{12}}{F_{12}}\right)^2 + \left(\frac{\delta F_{25}}{F_{25}}\right)^2} . \tag{3}$$

Similarly,

$$\delta R_{25/60} = \pm \frac{F_{25}}{F_{60}} \sqrt{\left(\frac{\delta F_{25}}{F_{25}}\right)^2 + \left(\frac{\delta F_{60}}{F_{60}}\right)^2} . \tag{4}$$

We compute expected photospheric ratios ($R^*_{12/25}$ and $R^*_{25/60}$) using the MSC spectral types and blackbodies corresponding to the stellar effective temperatures determined by Gray & Corbally (1994). Discrepancies at significance levels greater than 1 σ between the observed and the expected ratios therefore occur when

$$\frac{\Delta_{12/25}}{\delta_{\rm obs}} \equiv \frac{R_{12/25} - R^*_{12/25}}{\delta R_{12/25}} < -1 \tag{5}$$

and/or

$$\frac{\Delta_{25/60}}{\delta_{\rm obs}} \equiv \frac{R_{25/60} - R^*_{25/60}}{\delta R_{25/60}} < -1 . \tag{6}$$

In other words, we claim that one or more of the observed flux densities significantly exceed expectation for a dust-free stellar photosphere if either or both of the inequalities in equations (5) and (6) are satisfied. (We do not use any flux density with an FSC quality flag of 1, regardless of the ratio of the flux density and its listed 1 σ uncertainty.) Note that we implicitly *assume* that all MSC spectral types are free of error, so that

$$\delta R^*_{12/25} = \delta R^*_{25/60} = 0 . \tag{7}$$

We note that the blackbody photospheric flux ratios that we adopted for our comparisons correspond to monochromatic flux density ratios at the standard wavelengths of the *IRAS* filters, rather than to the in-band flux ratios for the *IRAS* filters. However, for a 5000 K blackbody the 12 and 25 μm monochromatic flux ratio is 4.084, while the in-band flux ratio is 4.172 (*IRAS* Explanatory Supplement 1988), which differ by only by a factor of 1.021, while for a 10,000 K blackbody the ratios are 4.225 and 4.345, differing by only a factor of 1.028. Not only are these differences of less than 3% between the blackbody monochromatic and in-band flux ratios very much smaller than the deviations exhibited by the sources found to have excesses (see Fig. 1), but our requirement for an excess relative to blackbody monochromatic flux density ratios is more conservative than comparing to blackbody in-band flux ratios, since slightly more emission is required from a star at the longer wavelength before it is classified as having an excess. The same remarks apply to the 25/60 μm blackbody flux ratio criterion. We also note that Kurucz LTE model atmospheres for A-type stars predict photospheric infrared energy distributions that are even slightly more steep than for blackbodies, e.g., the 9850 K, log $g = 4.25$ model for Sirius presented by Cohen et al. (1992) predicts 12/25 μm

[1] 18,956 stars from the 36,382 stars of Volume 1.

[2] Only raw FSC flux densities are used: i.e., we attempt no bandpass color corrections in the absence of prior knowledge of the temperature distribution of all material contributing to any excess infrared emission from a given source.

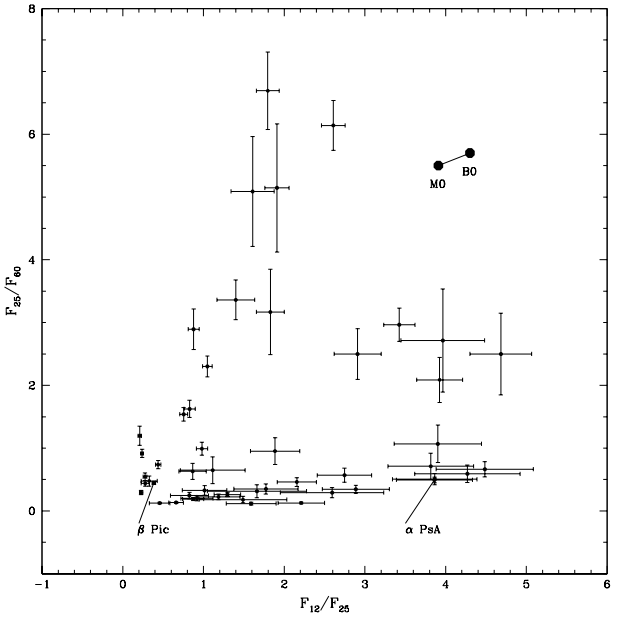

FIG. 1.—Diagrammatic comparison of flux density ratios for all sources (new and previously recognized) that have excellent- or moderate-quality FSC measurements in *each* of the three 12, 25, and 60 μm bands, and for which at least one of the ratios departs from the photospheric value at the 3 σ level or more. Ratios for main-sequence photospheres are indicated at the top right for stars with spectral types from M0 to B0.

monochromatic and in-band flux ratios of 4.325 and 4.558, respectively. Thus our requirement for longer wavelength excesses to be relative to photospheric blackbody monochromatic flux ratios is the most conservative of the above set that could have been adopted.

It is important to be clear about what will be accepted or rejected by this simple algorithm, and to check that we are neither falsely accepting spurious IR-excess sources nor incorrectly rejecting true excess sources. Since we are simply taking ratios of flux densities and then comparing them to the ratios expected for a star of given spectral type, we can easily enumerate all conceivable outcomes. Note that in the following we refer to the continuum spectral energy distribution (SED) of a given star. In no case have we computed and fitted a SED to a set of FSC flux densities: we compare *ratios* of flux densities and are therefore not concerned with absolute values. We simply list each of the ways in which the FSC fluxes can, *in principle*, exhibit ratios that are either consistent or inconsistent with expectation for a stellar SED.

3.3.1. *Rejected Sources*

There are only three cases that can, in principle, lead to the observed and expected ratios being consistent, and both of the two cases that could actually occur in practice would justify rejection of a source (i.e., there should be no false rejections):

Case 1.—The FSC flux densities are consistent with expectation for the stellar SED. The ratios would, of course, also be consistent with expectation, so that the star would be correctly rejected by our test.

Case 2.—The observed flux density ratio is consistent with expectation, *and* all FSC flux densities are in fact significantly above the stellar SED at mid- and far-IR wavelengths. This can occur only if FSC fluxes are dominated by emission from a second source at a similar temperature, thereby excluding thermal emission from grains, which will be much cooler. The second source would most likely be a star, which could be either a companion to the star in question, or a field star within the *IRAS* beams. Again, our ratio test would correctly reject the source.

Case 3.—The observed flux density ratio is consistent with expectation, *and* the FSC flux densities are significantly below the stellar SED; although conceivable, this case cannot arise in practice since it would require a deficit in the *stellar* SED at mid-IR wavelengths.

3.3.2. *Accepted Sources*

Similarly, there are only three cases that can, in principle, lead to a significant difference between the observed and expected ratios, and both of the two cases that could actually occur in practice would demand that a source be accepted (i.e., there should be no falsely accepted sources):

Case 4.—A significant discrepancy exists between the observed and the expected flux density ratios, and the 12, 25, and 60 μm FSC fluxes are in fact above the stellar SED. Assuming that the MSC and FSC sources are physically associated (and are not distinct sources that are coincidentally within the *IRAS* beam), the source is correctly accepted by our ratio test. The implication would also be that excess emission begins at a wavelength shortward of 12 μm.

Case 5.—A significant discrepancy exists between the observed and expected flux density ratios, but the 12 μm flux *is* consistent with the stellar SED. This implies that excess emission begins longward of $\lambda = 12$ μm, but the source would nonetheless be correctly accepted by our test. Similarly, for the (rare) case where FQUAL = 1 at 12 μm but there are good measurements at 25 and 60 μm, there could be a significant discrepancy between the observed and expected 25:60 μm ratios, while the 25 μm flux *is* consistent with the stellar SED. This would imply excess emission beginning longward of 25 μm, but we would again accept the source correctly.

Case 6.—A significant discrepancy exists between the observed and expected flux density ratios, and one or more FSC flux densities are below the stellar SED. As for case 3 above, this scenario cannot arise in practice since it would again require a deficit in the mid-IR region of the photospheric SED.

4. RESULTS

Our selection criteria compel us to reject 99.9% of 112,971 stars in the MSC, leaving a total of 127 stars.[3] (The breakdown by MSC volume is 35 stars from Volume 1, 27 from Volume 2, 32 from Volume 3, and 33 from Volume 4.) Some 108 of these sources are candidate main-sequence stars with debris disks. (The remainder are classical Be stars: see below.) Of these, a subset of 73 stars were not identified during the previous searches summarized in § 2. These "new" Vega-like sources are listed in Table 2. A total of 60 of these new stars exhibit discrepancies between observed and expected flux density ratios at greater than the 3 σ level. The 35 previously known MSC Vega-like stars are shown in Table 3. In Table 4 we list a further 12 stars

[3] In two instances, a single FSC source was found to be associated with two MSC stars that otherwise satisfied all the selection criteria; this occurred for the pair HD 24071 and HD 24072, and for the pair HD 35722 and HD 35736. These stars have been omitted.

TABLE 2

NEWLY IDENTIFIED CANDIDATE MAIN-SEQUENCE STARS WITH DEBRIS DISKS

Number (1)	HD (2)	SAO (3)	HR (4)	Name (5)	Spectral Type (6)	FQUAL (7)	F_{12} (Jy) (8)	F_{25} (Jy) (9)	F_{60} (Jy) (10)	F_{100} (Jy) (11)	$\Delta_{12/25}/\delta^{a}_{obs}$ (12)	$\Delta_{25/60}/\delta^{a}_{obs}$ (13)
1[b].....	7151	215402	...	...	F6 V	3311	3.880 ± 0.233	1.590 ± 0.111	0.355 ± 0.110	0.437 ± 0.131	−7.52	0.00
2.....	17848	248656	852	ν Hor	A2 V	3331	0.414 ± 0.021	0.097 ± 0.014	0.164 ± 0.030	0.490 ± 0.098	0.10	−37.40
3.....	21563	248797	1053	...	A3/5 V + G0/5	3311	0.585 ± 0.023	0.161 ± 0.013	0.088 ± 0.014	0.421 ± 0.067	−1.69	0.00
4.....	28001	233498	...	...	A4 V	3232	0.083 ± 0.012	0.070 ± 0.012	0.314 ± 0.031	0.660 ± 0.119	−11.14	−122.76
5[b].....	31925	150052	1604	...	F5 V	3311	0.629 ± 0.038	0.188 ± 0.032	0.187 ± 0.045	0.944 ± 0.217	−1.31	0.00
6.....	38206	150739	1975	...	A0 V	3231	0.195 ± 0.023	0.110 ± 0.021	0.313 ± 0.038	0.511 ± 0.123	−6.11	−67.27
7.....	38385	196116	1981	...	F3 V	3311	0.285 ± 0.020	0.095 ± 0.013	0.101 ± 0.018	0.345 ± 0.059	−2.41	0.00
8.....	38905	217529	...	...	F6/7 V	1231	0.091 ± 0.019	0.063 ± 0.017	0.174 ± 0.033	0.359 ± 0.061	0.00	−43.69
9.....	39944	171003	...	...	G1 V	1332	0.084 ± 0.019	0.153 ± 0.017	0.978 ± 0.049	1.790 ± 0.143	0.00	−287.63
10[c].....	41742	217706	2158	...	F5 V	3311	0.578 ± 0.040	0.164 ± 0.023	0.181 ± 0.036	1.310 ± 0.262	−1.11	0.00
11.....	42137	196509	...	...	K3/4 V	3311	1.090 ± 0.055	0.303 ± 0.021	0.238 ± 0.052	1.160 ± 0.255	−1.50	0.00
12.....	43954	151337	...	...	A0 V	2321	0.082 ± 0.021	0.180 ± 0.020	1.440 ± 0.072	1.660 ± 0.398	−29.24	−366.72
13.....	43955	151334	2266	...	B2/3 V	3321	0.147 ± 0.026	0.145 ± 0.030	0.442 ± 0.044	1.460 ± 0.336	−11.62	−70.54
14.....	46171	...	...	...	F3 V	3311	1.920 ± 0.096	0.566 ± 0.045	0.194 ± 0.045	0.959 ± 0.201	−2.34	0.00
15[b].....	49336	197195	2510	V339 Pup	B3 Vne	3311	0.239 ± 0.024	0.174 ± 0.023	0.172 ± 0.036	1.090 ± 0.207	−12.79	0.00
16[d].....	52140	197432	2621	...	B3 V	3311	0.586 ± 0.035	0.165 ± 0.020	0.119 ± 0.026	1.400 ± 0.308	−1.48	0.00
17.....	53143	249700	...	...	K1 V	3321	0.412 ± 0.021	0.108 ± 0.014	0.152 ± 0.040	0.670 ± 0.121	−0.50	−23.54
18.....	53376	197519	...	...	F3/5 V	3311	0.694 ± 0.042	0.261 ± 0.026	0.206 ± 0.045	1.900 ± 0.399	−4.78	0.00
19.....	53833	...	...	...	A9/F0 V	3311	0.240 ± 0.022	0.128 ± 0.020	0.368 ± 0.074	3.240 ± 0.616	−6.64	0.00
20.....	53842	258455	...	...	F5 V	3231	0.140 ± 0.015	0.054 ± 0.012	0.185 ± 0.031	1.810 ± 0.253	−2.33	−63.74
21.....	54096	218439	...	...	F5 V	3311	1.130 ± 0.057	0.530 ± 0.027	0.173 ± 0.033	0.767 ± 0.146	−13.28	0.00
22.....	56192	218555	...	...	B9/A0 V	1321	0.068 ± 0.013	0.136 ± 0.016	0.254 ± 0.069	1.850 ± 0.315	0.00	−32.46
23.....	60842	256416	...	...	A2/3 V	3321	22.900 ± 0.916	8.780 ± 0.351	1.430 ± 0.072	1.500 ± 0.240	−10.72	1.24
24.....	61950	249895	...	...	B8 V	3231	0.116 ± 0.012	0.073 ± 0.012	0.622 ± 0.037	2.180 ± 0.327	−8.73	−278.36
25.....	66591	250069	3159	...	B4 V	3321	0.276 ± 0.017	0.128 ± 0.012	0.278 ± 0.033	0.903 ± 0.144	−8.98	−75.80
26.....	67199	250088	...	...	K1 V	3311	0.361 ± 0.022	0.115 ± 0.021	0.169 ± 0.027	1.150 ± 0.161	−1.58	0.00
27.....	71397	...	...	...	F3 V	3321	7.260 ± 0.290	2.120 ± 0.085	0.715 ± 0.057	1.500 ± 0.330	−3.70	−10.00
28.....	73390	236105	3415	e01 Car	B4 V	3322	0.245 ± 0.022	0.189 ± 0.017	0.727 ± 0.051	1.320 ± 0.370	−17.90	−183.38
29.....	73752	176226	3430	...	G3/5 V	3321	1.780 ± 0.071	0.380 ± 0.027	0.152 ± 0.038	0.549 ± 0.126	1.54	−4.76
30.....	75416	256543	3502	η Cha	B8 V	3311	0.299 ± 0.030	0.133 ± 0.019	0.126 ± 0.028	1.010 ± 0.222	−5.11	0.00
31.....	80459	250521	...	...	B6 Vne	3311	0.287 ± 0.020	0.146 ± 0.016	0.112 ± 0.021	0.928 ± 0.158	−8.87	0.00
32.....	80950	256600	3721	...	A0 V	3311	0.212 ± 0.025	0.138 ± 0.019	0.122 ± 0.026	0.924 ± 0.176	−9.42	0.00
33.....	81515	200341	...	...	A5 V	3311	1.530 ± 0.092	0.982 ± 0.059	0.311 ± 0.100	2.820 ± 0.846	−19.80	0.00
34.....	88955	221895	4023	q Vel	A1 V	3311	1.300 ± 0.078	0.356 ± 0.032	0.148 ± 0.041	0.856 ± 0.214	−1.38	0.00
35.....	91375	256722	4138	...	A1 V	3321	0.605 ± 0.030	0.155 ± 0.020	0.145 ± 0.036	1.090 ± 0.229	−0.54	−15.24
36.....	99046	202396	...	...	F0 V	3311	2.310 ± 0.139	0.673 ± 0.054	0.278 ± 0.089	1.300 ± 0.377	−2.10	0.00
37[d].....	99211	156661	4405	γ Crt	A9 V	3321	1.550 ± 0.078	0.391 ± 0.047	0.144 ± 0.040	0.456 ± 0.119	−0.38	−3.53
38.....	100786	239204	...	...	A5 V	3311	2.220 ± 0.111	1.280 ± 0.077	0.293 ± 0.067	1.050 ± 0.231	−18.02	0.00
39[d].....	105686	203183	4628	...	A0 V	2231	0.201 ± 0.044	0.121 ± 0.036	0.384 ± 0.054	1.010 ± 0.313	−4.12	−51.27
40.....	108483	223454	4743	σ Cen	B2 V	3311	0.520 ± 0.031	0.165 ± 0.023	0.296 ± 0.071	1.440 ± 0.302	−2.33	0.00

TABLE 2—*Continued*

Number (1)	HD (2)	SAO (3)	HR (4)	Name (5)	Spectral Type (6)	FQUAL (7)	F_{12} (Jy) (8)	F_{25} (Jy) (9)	F_{60} (Jy) (10)	F_{100} (Jy) (11)	$\Delta_{12/25}/\delta^{a}_{obs}$ (12)	$\Delta_{25/60}/\delta^{a}_{obs}$ (13)
41	110058	223581	...	...	A0 V	1321	0.094 ± 0.023	0.266 ± 0.029	0.368 ± 0.063	1.150 ± 0.253	0.00	−33.76
42	114981	204273	...	...	B3/5 (V)ne	3231	0.156 ± 0.037	0.140 ± 0.038	0.216 ± 0.041	0.738 ± 0.184	−7.80	−23.61
43[b]	117360	257060	5082	S Cha	F5 V	3311	0.399 ± 0.056	0.182 ± 0.033	0.243 ± 0.058	2.120 ± 0.488	−3.88	0.00
44	120095	224440	...	...	B9/A0 V	3322	0.225 ± 0.038	0.810 ± 0.057	1.840 ± 0.129	1.340 ± 0.281	−77.08	−120.01
45	121617	224570	...	...	A1 V	1321	0.127 ± 0.032	0.692 ± 0.048	1.840 ± 0.129	2.450 ± 0.564	0.00	−141.88
46[e]	123247	224703	...	...	B9.5 V	3311	0.133 ± 0.025	0.156 ± 0.025	0.513 ± 0.128	4.400 ± 1.012	−15.85	0.00
47[d]	123356	...	...	...	G1 V	3311	1.250 ± 0.088	0.516 ± 0.108	0.152 ± 0.038	0.618 ± 0.154	−3.14	0.00
48	128760	225102	...	...	F8/G0 V	3311	1.250 ± 0.063	0.409 ± 0.037	0.192 ± 0.046	1.290 ± 0.297	−3.39	0.00
49	129364	225147	...	...	F5 V	3321	3.380 ± 0.169	1.770 ± 0.106	0.344 ± 0.065	1.190 ± 0.297	−14.92	−0.46
50	131885	183025	...	...	A0 V	1231	0.106 ± 0.028	0.214 ± 0.056	0.352 ± 0.053	1.070 ± 0.278	0.00	−27.71
51	137751	...	...	...	F6 V	3311	1.120 ± 0.056	0.630 ± 0.050	0.312 ± 0.062	2.500 ± 0.500	−14.03	0.00
52	139365	183649	5812	τ Lib	B2.5 V	3311	0.788 ± 0.039	0.299 ± 0.048	1.580 ± 0.363	8.880 ± 1.954	−3.69	0.00
53	139450	206837	...	...	G0/1 V	3311	0.548 ± 0.033	0.756 ± 0.053	0.692 ± 0.138	30.200 ± 6.040	−50.65	0.00
54	142165	183900	5906	...	B5 V	3311	0.271 ± 0.033	0.405 ± 0.049	7.610 ± 1.598	57.300 ± 11.460	−31.48	0.00
55[d]	143018	183987	5944	π Sco	B1 V + B2 V	2321	3.910 ± 0.235	8.930 ± 0.447	12.100 ± 0.847	27.900 ± 6.417	−112.51	−78.05
56	145263	184196	...	...	F0 V	2311	0.433 ± 0.069	0.515 ± 0.077	1.620 ± 0.405	3.490 ± 0.803	−17.97	0.00
57	145482	184221	6028	13 Sco	B2 V	2311	0.660 ± 0.053	1.540 ± 0.139	11.800 ± 2.950	19.200 ± 4.800	−74.45	0.00
58	153968	253795	...	...	F0 V	3311	0.367 ± 0.033	0.200 ± 0.026	0.303 ± 0.073	2.130 ± 0.490	−7.99	0.00
59	165088	...	...	...	F5 V	3321	23.000 ± 2.070	14.300 ± 2.002	2.810 ± 0.281	9.180 ± 2.387	−9.44	−0.60
60[d]	166841	254196	6808	...	B8/9 V	2231	0.134 ± 0.035	0.090 ± 0.023	0.500 ± 0.060	1.650 ± 0.380	−4.97	−107.00
61	172776	...	...	...	B9 V	3311	1.970 ± 0.118	1.240 ± 0.087	0.361 ± 0.094	1.420 ± 0.341	−17.93	0.00
62	176363	...	...	...	A2 V	3311	1.290 ± 0.219	0.635 ± 0.114	0.237 ± 0.057	2.460 ± 0.541	−4.29	0.00
63	176638	229461	7188	ζ CrA	B9/A0 V	3321	0.577 ± 0.046	0.306 ± 0.043	0.321 ± 0.055	1.120 ± 0.258	−7.66	−22.47
64	181296	246055	7329	η Tel	A0 V	3331	0.481 ± 0.024	0.491 ± 0.025	0.495 ± 0.045	0.435 ± 0.083	−46.57	−45.75
65	181327	246056	...	...	F5/6 V	3332	0.164 ± 0.018	0.248 ± 0.020	1.860 ± 0.074	1.720 ± 0.206	−38.61	−459.49
66	181869	229659	7348	α Sgr	B8 V	3311	0.807 ± 0.040	0.280 ± 0.036	0.123 ± 0.028	0.641 ± 0.141	−3.34	0.00
67	184800	246196	...	...	A8/9 V	3311	1.200 ± 0.072	0.415 ± 0.033	0.196 ± 0.049	0.522 ± 0.120	−4.40	0.00
68	191089	188955	...	...	F5 V	2231	0.111 ± 0.029	0.339 ± 0.051	0.711 ± 0.057	0.328 ± 0.079	−38.73	−63.37
69	200800	254944	...	...	A3 V	3311	0.774 ± 0.054	0.309 ± 0.022	0.150 ± 0.036	0.341 ± 0.068	−6.77	0.00
70[b,f]	203608	254999	8181	γ Pav	F7 V	3321	2.950 ± 0.118	0.642 ± 0.039	0.172 ± 0.036	0.522 ± 0.104	1.41	−2.30
71	206310	258915	...	...	F3 V	1231	0.083 ± 0.016	0.063 ± 0.014	0.516 ± 0.041	3.830 ± 0.728	0.00	−185.74
72	212283	213783	...	...	F3/5 V	3332	12.500 ± 0.625	6.960 ± 0.418	1.040 ± 0.073	0.604 ± 0.133	−16.72	1.74
73[b]	214953	231257	8635	...	G0 V	3311	0.604 ± 0.042	0.198 ± 0.030	0.152 ± 0.036	0.593 ± 0.130	−2.10	0.00

[a] Defined in eqs. (5) and (6); a null entry signifies inadequate data quality.
[b] Flagged by SIMBAD as a variable star.
[c] Has a K4 companion star (Corbally 1984).
[d] Flagged by SIMBAD as a double or mutiple star.
[e] Member of stellar cluster.
[f] λ Boo star (e.g., King 1994).

TABLE 3

MSC VEGA-LIKE STARS IDENTIFIED BOTH IN OUR SEARCH AND IN PREVIOUS SURVEYS

Number (1)	HD (2)	SAO (3)	HR (4)	Name (5)	Spectral Type (6)	FQUAL (7)	F_{12} (Jy) (8)	F_{25} (Jy) (9)	F_{60} (Jy) (10)	F_{100} (Jy) (11)	$\Delta_{12/25}/\delta^{a}_{obs}$ (12)	$\Delta_{25/60}/\delta^{a}_{obs}$ (13)
1[b]	3003	248208	136	β3 Tuc	A0 V	3311	0.446 ± 0.031	0.343 ± 0.027	0.190 ± 0.040	0.394 ± 0.079	−21.02	0.00
2	9672	147886	451	49 Cet	A1 V	3332	0.335 ± 0.034	0.384 ± 0.042	2.020 ± 0.121	1.880 ± 0.207	−25.64	−229.57
3	10647	232501	506	q1 Eri	F8 V	3332	0.814 ± 0.049	0.282 ± 0.037	0.815 ± 0.106	1.080 ± 0.173	−2.99	−82.66
4	10700	147986	509	τ Cet	G8 V	3231	9.220 ± 0.553	2.160 ± 0.173	0.484 ± 0.053	0.870 ± 0.270	0.41	−1.84
5	10800	258271	512	...	G1/2 V	3311	0.681 ± 0.041	0.243 ± 0.022	0.173 ± 0.031	1.240 ± 0.211	−4.30	0.00
6[b]	16157	215947	...	CC Eri	M0 Vp	3311	0.494 ± 0.025	0.155 ± 0.020	0.096 ± 0.020	0.213 ± 0.043	−1.73	0.00
7[c]	27290	233457	1338	γ Dor	F0 V	3331	1.680 ± 0.067	0.428 ± 0.026	0.205 ± 0.033	0.488 ± 0.102	−0.81	−9.92
8[b]	33949	150239	1705	κ Lep	B7 V	3321	0.541 ± 0.027	0.197 ± 0.022	0.346 ± 0.055	1.640 ± 0.328	−4.48	−46.26
9	38393	170759	1983	γ Lep A	F7 V	3331	4.400 ± 0.220	0.981 ± 0.059	0.228 ± 0.036	0.483 ± 0.116	1.02	−1.78
10	38678	150801	1998	ζ Lep	A2 Vann	3331	2.120 ± 0.106	1.160 ± 0.093	0.366 ± 0.073	1.000 ± 0.240	−13.70	−3.64
11	39060	234134	2020	β Pic	A5 V	3332	3.390 ± 0.136	8.810 ± 0.352	19.700 ± 0.788	11.000 ± 0.440	−174.13	−205.35
12	40136	150957	2085	η Lep	F1 V	3321	2.880 ± 0.115	0.726 ± 0.036	0.212 ± 0.047	1.650 ± 0.380	−0.72	−2.85
13	61712	218858	...	...	B7/8 V	3311	5.110 ± 0.358	2.880 ± 0.202	2.000 ± 0.400	14.100 ± 2.679	−14.00	0.00
14	69830	154093	3259	...	K0 V	3311	0.967 ± 0.058	0.341 ± 0.038	0.216 ± 0.056	1.120 ± 0.291	−3.52	0.00
15[b]	80951	256599	3720	...	A1 V	3322	0.442 ± 0.031	0.200 ± 0.022	1.570 ± 0.079	2.720 ± 0.354	−6.90	−359.32
16	93331	156211	...	...	B9.5 V	2232	0.137 ± 0.029	0.166 ± 0.032	0.677 ± 0.061	1.240 ± 0.248	−14.48	−105.18
17[b]	98800	179815	...	...	K4 V	3232	1.980 ± 0.119	9.440 ± 0.755	7.890 ± 0.789	4.570 ± 0.320	−183.22	−28.44
18[c]	107439	223370	...	SX Cen	G3/5 Vp	3321	4.940 ± 0.790	3.530 ± 0.176	1.050 ± 0.084	3.230 ± 0.678	−11.52	−7.02
19[c]	109085	157345	4775	η Crv	F2 V	3331	2.240 ± 0.134	0.770 ± 0.062	0.308 ± 0.043	0.803 ± 0.249	−4.26	−7.75
20[b]	113766	223904	...	...	F3/5 V	3321	1.580 ± 0.095	1.800 ± 0.090	0.622 ± 0.062	1.030 ± 0.258	−47.60	−8.42
21	115892	204371	5028	ι Cen	A2 V	3321	3.600 ± 0.216	0.973 ± 0.097	0.195 ± 0.045	0.700 ± 0.168	−1.14	−0.53
22	121847	182134	5250	47 Hya	B8 V	3232	0.235 ± 0.031	0.256 ± 0.044	1.280 ± 0.115	2.300 ± 0.230	−16.82	−142.35
23[b]	135344	206462	...	...	A0 V	3322	1.570 ± 0.079	6.910 ± 0.484	23.600 ± 2.124	23.200 ± 1.392	−203.55	−160.89
24	139614	226057	...	...	A7 V	3322	4.140 ± 0.207	17.300 ± 0.865	18.900 ± 0.945	12.100 ± 1.452	−232.17	−72.95
25	142096	183895	5902	λ Lib	B3 V	3321	0.488 ± 0.034	0.564 ± 0.102	0.895 ± 0.090	1.790 ± 0.358	−20.29	−39.07
26[b]	142114	183896	5904	2 Sco	B2.5 Vn	3321	0.649 ± 0.039	2.350 ± 0.141	4.310 ± 0.388	11.500 ± 2.300	−170.18	−87.50
27	142666	183956	...	...	A8 V	3322	8.670 ± 0.347	11.500 ± 0.575	7.470 ± 0.373	5.120 ± 0.973	−70.65	−37.62
28	144432	184124	...	...	A9/F0 V	2321	7.630 ± 0.458	9.230 ± 0.554	5.680 ± 0.341	8.120 ± 2.030	−47.54	−29.06
29[d]	150193	184536	...	...	A1 V	3321	17.500 ± 0.700	16.700 ± 0.668	7.250 ± 0.435	12.500 ± 2.125	−53.14	−20.20
30[b,e]	176269	210815	7169	...	B7/8 V	3311	0.438 ± 0.044	0.655 ± 0.052	6.390 ± 1.597	54.400 ± 13.056	−41.62	0.00
31[e]	178253	210990	7254	α CrA	A0/1 V	3311	1.010 ± 0.061	0.348 ± 0.049	0.245 ± 0.059	2.750 ± 0.578	−2.95	0.00
32	195627	254823	7848	ϕ01 Pav	F0 V	3331	1.020 ± 0.061	0.264 ± 0.032	0.522 ± 0.068	1.800 ± 0.432	−0.56	−57.24
33	207129	230846	8323	...	G0 V	3331	0.897 ± 0.054	0.200 ± 0.024	0.301 ± 0.042	0.715 ± 0.186	0.62	−40.25
34[c]	216956	191524	...	α PsA	A3 V	3332	18.500 ± 1.850	4.790 ± 0.335	9.690 ± 0.581	10.900 ± 0.654	−0.68	−113.07
35	224392	255609	9062	η Tuc	A1 V	3311	0.477 ± 0.029	0.136 ± 0.019	0.133 ± 0.028	0.454 ± 0.091	−1.29	0.00

[a] Defined in eqs. (5) and (6); a null entry signifies inadequate data quality.
[b] Flagged by SIMBAD as a double or mutiple star.
[c] Flagged by SIMBAD as a variable star.
[d] Classed as Herbig Ae star by Finkenzeller & Mundt 1984.
[e] Located in R CrA star-forming region.

TABLE 4

VEGA-LIKE CANDIDATES WITH UNCERTAIN LUMINOSITY CLASSIFICATION

Number (1)	HD (2)	SAO (3)	HR (4)	Name (5)	Spectral Type (6)	FQUAL (7)	F_{12} (Jy) (8)	F_{25} (Jy) (9)	F_{60} (Jy) (10)	F_{100} (Jy) (11)	$\Delta_{12/25}/\delta^{a}_{obs}$ (12)	$\Delta_{25/60}/\delta^{a}_{obs}$ (13)
1[d]	11995	248464	571	...	F0 IV/V	3311	0.330 ± 0.020	0.102 ± 0.016	0.079 ± 0.016	0.252 ± 0.048	−1.66	0.00
2	12363	255835	593	σ Hyi	F5/6 IV/V	3311	0.359 ± 0.022	0.122 ± 0.024	0.121 ± 0.022	0.470 ± 0.080	−1.94	0.00
3[b,d]	27604	233476	1365	...	F7 IV/V	3311	0.394 ± 0.028	0.113 ± 0.017	0.098 ± 0.020	0.431 ± 0.082	−1.11	0.00
4[b,d]	34798	150335	1753	...	B5 IV/V	2232	0.077 ± 0.021	0.085 ± 0.020	0.206 ± 0.033	0.643 ± 0.180	−10.13	−44.35
5[d]	37104	150588	...	...	B5 IV/V	1231	0.080 ± 0.019	0.079 ± 0.021	0.266 ± 0.040	1.050 ± 0.252	0.00	−60.35
6[d]	45610	196834	...	...	G3 IV/V(W)	3311	0.450 ± 0.027	0.156 ± 0.028	0.093 ± 0.019	1.070 ± 0.225	−2.22	0.00
7[d]	97495	222639	4350	...	A3 IV/V	3311	0.383 ± 0.050	0.147 ± 0.025	0.208 ± 0.046	1.230 ± 0.271	−2.83	0.00
8[b,c,d]	149367	184475	...	...	B8/9 IV/V	2311	2.750 ± 0.138	1.280 ± 0.090	0.953 ± 0.191	4.540 ± 0.863	−11.23	0.00
9	159492	244896	6549	π Ara	A5 IV/V	3311	0.460 ± 0.041	0.243 ± 0.036	0.315 ± 0.079	1.630 ± 0.391	−6.89	0.00
10	160691	244981	6585	μ Ara	G3 IV/V	2311	1.540 ± 0.108	0.449 ± 0.063	0.352 ± 0.088	2.440 ± 0.586	−1.25	0.00
11	172555	254358	7012	...	A5 IV/V	3331	1.520 ± 0.061	1.090 ± 0.055	0.306 ± 0.046	0.991 ± 0.218	−31.14	−3.69
12[d]	219571	247814	8848	γ Tuc	F3 IV/V	3331	2.940 ± 0.147	0.678 ± 0.034	0.171 ± 0.032	0.273 ± 0.055	0.64	−2.12

[a] Defined in eqs. (5) and (6); a null entry signifies inadequate data quality.
[b] Flagged by SIMBAD as a double or multiple star.
[c] Member of Sco-Cen OB association (e.g., de Geus, de Zeeuw, & Lub 1989).
[d] Not identified in previous surveys of the *IRAS* database.

TABLE 5

CLASSICAL BE STARS EXTRACTED DURING OUR SEARCH FOR VEGA-LIKE SOURCES

Number (1)	HD (2)	SAO (3)	HR (4)	Name (5)	Spectral Type (6)	FQUAL (7)	F_{12} (Jy) (8)	F_{25} (Jy) (9)	F_{60} (Jy) (10)	F_{100} (Jy) (11)	$\Delta_{12/25}/\delta^{a}_{obs}$ (12)	$\Delta_{25/60}/\delta^{a}_{obs}$ (13)
1	28497	149674	1423	DU Eri	B2 (V)ne	3321	0.943 ± 0.047	0.443 ± 0.035	0.163 ± 0.037	0.648 ± 0.117	−10.67	−4.52
2	42054	196503	2170	...	B3/5 Vnn	3321	0.648 ± 0.032	0.362 ± 0.022	0.173 ± 0.036	0.490 ± 0.103	−17.64	−7.89
3	48917	197149	2492	FT CMa	B2 V	3311	1.140 ± 0.103	0.530 ± 0.032	0.231 ± 0.053	0.834 ± 0.167	−9.11	0.00
4	49131	197177	2501	HP CMa	B2 Vn	3311	0.694 ± 0.056	0.326 ± 0.026	0.147 ± 0.031	1.050 ± 0.210	−8.89	0.00
5	49319	197192	2507	...	B4 Vne	3321	0.197 ± 0.020	0.132 ± 0.018	0.192 ± 0.040	0.809 ± 0.178	−10.74	−28.86
6	50123	197263	2545	...	B3 V	3321	1.790 ± 0.072	0.584 ± 0.035	0.160 ± 0.043	0.846 ± 0.169	−5.39	−2.03
7	57150	197824	2787	NV Pup	B2 V + B3 IVne	3311	2.710 ± 0.108	1.490 ± 0.075	3.520 ± 0.774	2.550 ± 0.790	−21.06	0.00
8	66194	250055	3147	V374 Car	B3 Vn	3311	0.310 ± 0.025	0.158 ± 0.022	0.530 ± 0.127	2.160 ± 0.475	−7.25	0.00
9	81753	177461	3745	...	B5 V	3321	0.290 ± 0.041	0.172 ± 0.022	0.311 ± 0.050	1.810 ± 0.416	−7.94	−45.06
10	83754	155388	3849	κ Hya	B3/5 IV/V	3231	0.225 ± 0.027	0.128 ± 0.028	0.270 ± 0.041	1.180 ± 0.295	−5.67	−41.40
11	83953	177840	3858	I Hya	B5 V	3331	2.000 ± 0.100	1.050 ± 0.063	0.327 ± 0.043	0.649 ± 0.156	−15.72	−5.39
12	109857	256967	4804	...	B8 Vn	3311	0.305 ± 0.021	0.183 ± 0.016	0.276 ± 0.058	1.360 ± 0.272	−13.45	0.00
13	120324	224471	5193	μ Cen	B2 IV/Vne	3311	1.800 ± 0.144	0.733 ± 0.059	0.422 ± 0.110	1.670 ± 0.434	−6.53	0.00
14	124639	258697	5327	...	B8 V	3311	0.261 ± 0.018	0.127 ± 0.017	0.094 ± 0.016	0.659 ± 0.112	−7.15	0.00
15	124771	257142	5336	ϵ Aps	B3 V	3322	0.433 ± 0.026	1.220 ± 0.061	8.560 ± 0.428	13.000 ± 0.650	−140.72	−551.42
16	127972	225044	5440	η Cen	B1.5 Vn	3321	5.540 ± 0.277	1.890 ± 0.113	0.454 ± 0.068	2.510 ± 0.627	−5.89	−2.31
17	148184	159918	6118	χ Oph	B2 Vne	2321	11.300 ± 0.678	5.390 ± 0.323	2.870 ± 0.258	12.800 ± 3.200	−12.22	−18.87
18	153261	244362	6304	V828 Ara	B1 (V)ne	3311	0.661 ± 0.086	0.305 ± 0.040	0.271 ± 0.062	1.980 ± 0.416	−5.32	0.00
19	158503	244829	...	...	B(7) Vnnep	3311	0.579 ± 0.046	0.196 ± 0.033	0.238 ± 0.057	2.040 ± 0.510	−2.30	0.00
20	214748	191318	8628	ϵ PsA	B8 V	3311	1.110 ± 0.089	0.476 ± 0.081	0.296 ± 0.095	0.737 ± 0.221	−4.32	0.00
21	224686	255619	9076	ϵ Tuc	B8/9 V	3311	0.594 ± 0.036	0.212 ± 0.023	0.143 ± 0.033	0.355 ± 0.075	−4.05	0.00

[a] Defined in eqs. (5) and (6); a null entry signifies inadequate data quality.

that satisfy all of our selection criteria, but where the assignment by the MSC of a luminosity class of V is uncertain. Stars labeled by footnote "d" on their sequence numbers (col. [1] of Table 4) have not been identified in previous surveys of the *IRAS* catalogs. All other stars *were* found by one or more of the surveys listed in Table 1. In Table 5 we show 19 classical Be stars of class V that were extracted during our search (and identified using the SIMBAD database), plus two Be sources with uncertain luminosity classifications. We will not consider the classical Be stars any further. Stellar proper motions are not included in the MSC, but we have used proper motions listed in the SAO catalog to examine the optical coordinates of the stars in Tables 2 and 4 a posteriori, and thereby check for spurious positional associations of MSC stars and FSC IR sources. Resultant proper motions range from 0".1 to 41", with a mean value of just 5".2 during the interval of time separating the epoch of the coordinates in the HD catalog (or, for MSC stars at declinations south of $-53°$, the SAO catalog) and the epoch of the *IRAS* measurements. The separations of the proper-motion–corrected coordinates and the nominal coordinates of the FSC sources are less than 60" for all but two of the objects in Tables 2 and 4. The stars HD 184800 and HD 212283 are separated from their candidate FSC associations by 66".9 and 60".5, respectively. Formally, they would be rejected by our selection criteria (which stipulate separations up to 60") but, since they exceed the search radius only marginally, we will retain them in our sample here. Some eight stars listed in Table 2 have no entry in the SAO catalog; in the absence of knowledge of their proper motions, these source candidates should be regarded with caution. Note that relatively nearby, high proper-motion sources could conceivably have been rejected mistakenly, since cumulative proper motions were not determined for the full set of MSC stars prior to positional association with the FSC. Our survey is therefore likely biased to the detection of the more distant debris disk sources.

In each of Tables 2 to 5 we provide, in ascending order of HD number, our sequence number (col. [1]), the SAO and HR numbers (where applicable), the name of the star, the MSC spectral classification, the quality flags for the four *IRAS* bands, and the FSC flux densities with 1 σ uncertainties. (Stellar coordinates are readily obtainable from on-line archives such as SIMBAD.) Columns (12) and (13) contain, for each star, our measures of the significance of the discrepancies between the observed mid- to far-infrared flux density ratios and the expected photospheric values, given the MSC spectral type. These columns correspond, respectively, to the values computed for the left-hand sides of the inequalities in equations (5) and (6) derived earlier: null entries are made when the quality flag of either the 12 μm or the 25 μm flux density is equal to unity. Included in the two Tables are only those stars for which inequalities in equations (5) and/or (6) hold. Such restriction to the ≥ 1 σ criterion is hardly conservative, but we include all such sources so that, should the reader prefer, a higher cutoff level can be adopted and a subset of the sources taken. We will discuss only the ≥ 3 σ sources below.

Note that we accept stars of *all* spectral types that meet the criteria described in § 3, including 26 stars earlier than A0 with excesses ≥ 3 σ. In the absence of any knowledge of the interstellar environment of these luminous stars we have made no attempt to exclude them, although the reader should keep in mind the possibility that at least some of the excess IR emission from these sources could be due to the heating of local interstellar material.

We made a further inspection of the 60 sources in Table 2 with discrepancies between observed and expected ratios above the 3 σ level. Each source was examined using the on-line IRSKY facility provided by the Infrared Processing and Analysis Center, which we employed to confirm all of the FSC flux densities obtained via our catalog manipulation, and to determine whether or not any of the stars also have positional associations with PSC objects. We found that 38% of the 60 stars (23 sources) have no entry in the PSC. Of the remainder, 13 stars have just one PSC measurement with an FQUAL flag ≥ 2 at 12, 25, or 60 μm; 24 stars have two or three measurements in these bands with FQUAL > 1. There are many possible reasons why these latter stars were not identified during the surveys of the PSC. For example, 11 of the 24 stars have no entries in the SAO catalog and/or would have been filtered out by the criteria on FQUAL used by the two largest and most recent surveys, which we briefly discuss next.

5. COMPARISON TO PREVIOUS METHODS

We consider the methods used for two large surveys of the *IRAS* PSC by Stencel & Backman (1991) and Oudmaijer et al. (1992).

To obtain their sample from the SAO catalog, Stencel & Backman (1991) assumed that 12 μm flux densities listed in the PSC were photospheric in origin, and a test was then made for IR excesses by comparing observed flux densities at 25, 60, and 100 μm to values predicted using 12:25, 12:60, and 12:100 ratios for "normal" (dust-free) stars. As here, they used the errors on the flux densities to identify sources with significant excesses. However, to define photospheric ratios, they used median values of observed 12:25 μm ratios from their entire sample of position-associated stars, averaged over whole spectral type bands. These ratios were then used to derive equivalent color temperatures, with which 12:60 and 12:100 μm ratios were computed. Their 12:25 μm ratios for each spectral band (B, A, F, G, K, and M) turn out to be slightly less than would be predicted for blackbody emission. This is presumably due in part to the fact that some 7% of their sample of stars subsequently appear actually to have significant excess IR emission. They also speculate (cf., Cohen et al. 1987) that normal stars in general might have slight IR excesses.

Rather than attempt to determine photospheric ratios a priori and in a statistical fashion using a sample that would most likely include stars with circumstellar grains, we preferred to employ blackbody ratios, source-by-source, for each spectral subclass. We computed the photospheric ratios using the relatively accurate spectral types assigned by the MSC; Stencel & Backman (1991) adopted the less reliable spectral types listed in the SAO catalog, hence their use of whole spectral bands, although it must be noted that at far-IR wavelengths there is in fact little spread in the ratios across any given band. Note also that, since Stencel & Backman used the 12 μm flux density only to scale the predicted flux densities at 25, 60, and 100 μm and probe for excess emission in these latter bands, their sample could include stars with or without excess emission at 12 μm.

However, the Stencel & Backman (1991) technique could lead to some stars with genuine IR excesses nevertheless being rejected. First, a 12 μm flux that is in fact in excess of the photospheric value for a given star would of course lead

to an overestimation of the predicted photospheric 25 μm flux: it could sometimes happen that the flux measured at 25 μm is in reality also significantly above the photospheric level, but nonetheless at or below the high predicted value, which would lead to a false rejection of the star. We avoid this possibility in the present work by taking flux ratios, rather than using absolute values. Second, the demand for a 12 μm detection obviously excludes all sources that are detected with moderate or excellent quality *only* at 25 and 60 μm; such sources account for 6% of our final sample in Tables 2 and 3. A comparable fraction may have been missed by Stencel & Backman (1991).

Oudmaijer et al. (1992), like Stencel & Backman (1991), cross-correlated the SAO catalog with the *IRAS* PSC and searched for IR excesses from stars of various spectral types and luminosity classes. However, instead of comparing *IRAS* flux densities or flux density ratios directly, Oudmaijer et al. (1992) derived 12, 25, and 60 μm magnitudes, after which they inspected the resulting scatter in a [25] − [60], [12] − [25] diagram and searched for avoidance of the locus defined by photospheric colors.

6. DISCUSSION

In Figure 1 we plot F_{25}/F_{60} against F_{12}/F_{25} for the subset of 50 of the 108 new and previously identified Vega-like stars (Tables 2 and 3) that have excellent- or moderate-quality detections in *all* three of the 12, 25, and 60 μm bands, *and* for which at least one of the flux density ratios deviates from the computed photospheric value by 3 σ or more. The (short) locus for blackbody main-sequence photospheres is drawn at the top right of this diagram. Note that the handful of data points (four stars) with "forbidden" excursions either above or to the right of the main-sequence locus are nevertheless within 1 to 2 σ of it. Also, not surprisingly, given the proximity of all photospheric mid-IR SEDs to Rayleigh-Jeans curves, it becomes clear that the assumption in equation (7) concerning errors on the stellar spectral types is irrelevant for these sources, since they all have at least one ratio that avoids the *entire* main-sequence locus.

Two of the prototype Vega-like stars, β Pic and Fomalhaut (α PsA), were extracted during our search, and it can be seen that they both lie in well-populated regions of Figure 1: evidently, their mid- and far-IR colors are not unusual.

In Figure 2 we show a histogram of the 88 new and previously recognized MSC Vega-like stars with at least one flux density ratio that is discrepant with the photospheric value at the 3 σ level or higher. The abscissa is stellar effective temperature ($T_{\rm eff}$), and the sources are grouped into bins of width 0.1 dex. MSC spectral types were converted to temperatures using the calibrations by Gray & Corbally (1994). (Spectral types are shown along the top of Fig. 2.) The distribution of sources is seen to rise quickly with decreasing $T_{\rm eff}$, until we reach early A-type stars. There is a dip for late A stars (reflecting the smaller number of stars classified as such) followed by a second peak around G0, below which the distribution cuts off ($T_{\rm eff} < 4500$ K). The latter characteristic is most likely due to the limiting sensitivity of the measurements in the FSC rather than to a paucity of debris disks around stars of spectral type mid-G and later. Combining the data of Tables 2, 3, and 5, we find that 43 stars with spectral types earlier than B8 are selected by our criteria, of which 21 are classical Be stars (Table 5) with free-free excesses. The remaining B stars (in Tables 2 and 3) show excesses attributable to dust emission, although in the case of some of the more luminous early B-type stars (e.g., π Sco, 2 Sco, 13 Sco), this emission may arise from warm dust in surrounding reflection nebulae.

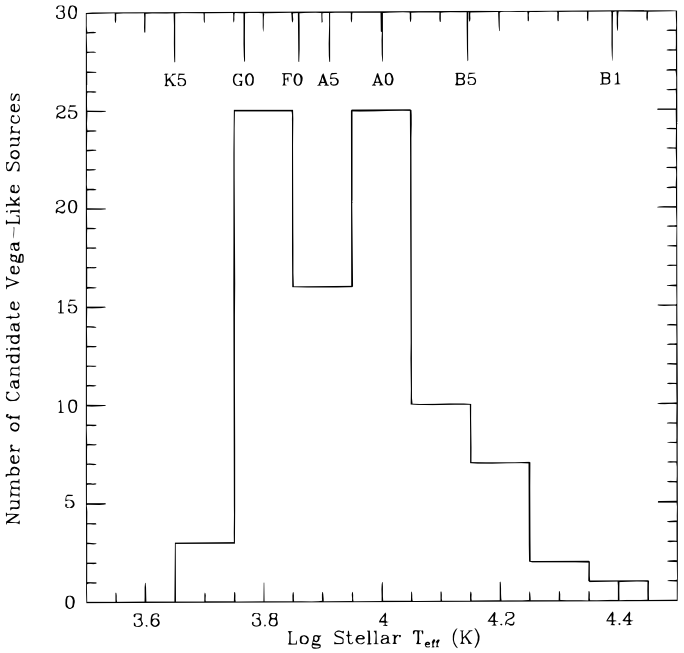

FIG. 2.—Histogram of the number of stars versus stellar effective temperature, for new and previously identified sources with at least one *IRAS* flux ratio that is discrepant by 3 σ or more with the expectation for a blackbody of the corresponding stellar effective temperature.

7. CONCLUSIONS

We have used the positions and luminosity classes of Southern Hemisphere sources listed in the Michigan Catalog of Two-dimensional Spectral Types for the HD Stars together with the positions, data-quality flags, and flux densities of mid- and far-IR sources in the *IRAS* Faint Source Survey Catalog to isolate a sample of main-sequence stars with possible excess IR emission, most likely indicative of thermal radiation from dust grains in associated debris disks. Our search criteria extracted a total of 108 main-sequence stars with possible IR excesses, 73 of which have not been previously identified. For some 60 of these "new" candidate Vega-like stars, measured IR flux density ratios and expected photospheric ratios are discrepant above the 3 σ level. Further analysis of a subset of the new sources will be made following near- to far-IR photometry with the *Infrared Space Observatory* and ground-based optical and IR photometry and spectroscopy.

V. M. was supported during the initial stages of this work by the UK Particle Physics and Astronomy Research Council, and currently by NASA grant NAGW-4030 from the Origins of Solar Systems program. We have made extensive use of the on-line facilities of the National Space Science Data Center at the NASA Goddard Space Flight Center, together with the SIMBAD database operated at CDS, Strasbourg, France. Many thanks are due to Anneila Sargent and Dana Backman for reading our manuscript. We also thank Alan Wood of the Rutherford Appleton Laboratory, UK, for his quick and helpful responses to our queries concerning the manipulation of data catalogs. We thank R. Oudmaijer and an anonymous referee for their comments on the paper.

REFERENCES

Aitken, D. K., Moore, T. J. T., Roche, P. F., Smith, C. H., & Wright, C. M. 1993, MNRAS, 265, L41
Aumann, H. H. 1985, PASP, 97, 885
Aumann, H. H., et al. 1984, ApJ, 278, L23
Aumann, H. H., & Probst, R. G. 1991, ApJ, 368, 264
Backman, D. E., & Paresce, F. 1993, in Protostars and Planets III, ed. E. H. Levy & J. I. Lunine (Tucson: Univ. Arizona Press), 1253
Cheng, K. P., Bruhweiler, F. C., Kondo, Y., & Grady, C. A. 1992, ApJ, 396, L83
Chini, R., Krügel, E., Shustov, B., Tutukov, A., & Kreysa, E. 1991, A&A, 252, 220
Cohen, M., Schwarz, D., Choksi, A., & Walker, R. 1987, AJ, 93, 1199
Cohen, M., Walker, R. G., Barlow, M. J., & Deacon, J. R. 1992, AJ, 104, 1650
Corbally, C. J. 1984, ApJS, 55, 657
Coté, J. 1987, A&A, 181, 77
de Geus, E. J., de Zeeuw, P. T., & Lub, J. 1989, A&A, 216, 44
Finkenzeller, U., & Mundt, R. 1984, A&AS, 55, 109
Gillett, F. C. 1986, in Light on Dark Matter, ed. F. P. Israel (Dordrecht: Reidel), 61
Gliese, W. 1969, Catalog of Nearby Stars (Heidelberg: Publ. Astr. Rechen Institute)
Gray, R. O., & Corbally, C. J. 1994, AJ, 107, 742
Houk, N. 1978, Michigan Catalog of Two-dimensional Spectral Types for the HD Stars, Vol. 2 (Ann Arbor: Univ. Michigan)
———. 1982, Michigan Catalog of Two-dimensional Spectral Types for the HD Stars, Vol. 3 (Ann Arbor: University of Michigan)
———. 1994, in PASP Conf. Ser. 60, The MK Process at 50 Years: A Powerful Tool for Astrophysical Insight, ed. C. J. Corbally, R. O. Gray, & R. F. Garrison (San Francisco: ASP), 285
Houk, N., & Cowley, A. P. 1975, Michigan Catalog of Two-dimensional Spectral Types for the HD Stars, Vol. 1 (Ann Arbor: Univ. Michigan)
Houk, N., & Smith-Moore, M. 1988, Michigan Catalog of Two-dimensional Spectral Types for the HD Stars, Vol. 4 (Ann Arbor: Univ. Michigan)
IRAS Catalogs and Atlases: Explanatory Supplement. 1988, ed. C. A. Beichman, G. Neugebauer, H. J. Habing, P. E. Clegg, & T. J. Chester (Washington, DC: GPO)
IRAS Point Source Catalog, Version 2. 1988, Joint *IRAS* Science Working Group (Washington, DC: GPO) (PSC)
Jaschek, M., Jaschek, C., & Egret, D. 1986, A&A, 158, 325
Johnson, H. 1986, ApJ, 300, 401
Kalas, P., & Jewitt, D. 1996, AJ, 111, 1347
———. 1997, Nature, 386, 52
King, J. R. 1994, MNRAS, 269, 209
Knacke, R. F., Fajardo-Acosta, S. B., Telesco, C. M., Hackwell, J. A., Lynch, D. K., & Russell, R. W. 1993, ApJ, 418, 440
Lagrange-Henri, A. M. 1995, Ap&SS, 223, 19
Moshir, M., et al. 1989, Explanatory Supplement to the *IRAS* Faint Source Survey (Pasadena: JPL) (FSC)
Odenwald, S. F. 1986, ApJ, 307, 711
Oudmaijer, R. D., van der Veen, W. E. C. J., Waters, L. B. F. M., Trams, N. R., Waelkens, C., & Engelsman, E. 1992, A&AS, 96, 625
Patten, B. M., & Willson, L. A. 1991, AJ, 102, 323
Sadakane, K., & Nishida, M. 1986, PASP, 98, 685
Skinner, C. J., Barlow, M. J., & Justtanont, K. 1992, MNRAS, 255, 31P
Skinner, C. J., Sylvester, R. J., Graham, J. R., Barlow, M. J., Meixner, M., Keto, E., Arens, J. F., & Jernigan, J. G. 1995, ApJ, 444, 861
Smith, B. A., Fountain, J. W., & Terrile, R. J. 1992, A&A, 261, 499
Smith, B. A., & Terrile, R. J. 1984, Science, 226, 1421
Stencel, R. E., & Backman, D. A. 1991, ApJS, 75, 905
Sylvester, R. J., Barlow, M. J., & Skinner, C. J. 1994a, MNRAS, 266, 640
———. 1994b, Ap&SS, 212, 261
Sylvester, R. J., Skinner, C. J., Barlow, M. J., & Mannings, V. 1996, MNRAS, 279, 915
Telesco, C. M., & Knacke, R. S. 1991, ApJ, 372, L29
Vidal-Madjar, A., & Ferlet, R. 1994, in Circumstellar Dust Disks and Planet Formation, ed. R. Ferlet & A. Vidal-Madjar (Paris: Editions Frontières), 7
Walker, H. J., & Wolstencroft, R. D. 1988, PASP, 100, 1509
Zuckerman, B., & Becklin, E. E. 1993, ApJ, 414, 793